A Strength Tensor Based Failure Criterion with Stress Interactions

Paul V. Osswald,[1] **Tim A. Osswald**[2]
[1]*Technical University of Munich, München, Germany*

[2]*University of Wisconsin-Madison, Madison, Wisconsin*

A 3D failure criterion for anisotropic materials that includes stress interactions is developed. The strength tensor model is based on the Gol'denblat–Kopnov criterion, where fourth order strength tensor stress interaction components are computed based on the slope of the failure surface at distinct stress axes intersections. Experimental data from the literature for unidirectional FRP's, an anisotropic paperboard material and textile reinforced composites are used to validate the model.
POLYM. COMPOS., 00:000–000, 2017.

INTRODUCTION

With the increased use of continuous, chopped and textile fiber reinforced polymer composites in the design and manufacture of critical parts and structures for the aerospace and automotive industries, interest in the strength and failure of these parts has been continually growing. In the past decades, various failure criteria models have been developed and modified. Some models were developed for unidirectional fiber reinforced composites and cannot be extended to model failure in systems neither with fiber orientation distributions nor textile reinforced composite structures. Furthermore, none of the existing models account for all modes of failure [1, 2], nor include all stress interactions, if any. Some only include interactions between normal stresses, such as the interaction between longitudinal and transverse normal stresses and others only include interactions between the transverse shear stress and transverse normal stress. It can also be said that up until recently, exposure of a specific model, and even acceptance, was often linked to geographical location of the engineer.

Today, there are two general families of failure criteria. The first and oldest one are strength tensor based criteria, which represent the failure surface with a single scalar function, such as the Tsai–Hill [3], the Gol'denblat–Kopnov [4], the Malmeister [5] or Tsai-Wu [6], and the Theocaris [7] criteria. In addition to the basic engineering failure strengths such as longitudinal and transverse strengths in tension and compression, as well as shear strengths, they include the interaction between longitudinal stress and transverse stress. Such models, such as the Tsai–Wu model, are widely used and have been incorporated into finite element analysis software to perform strength analysis of anisotropic parts. However, these models do not include the interaction between normal stresses and shear stresses, which dominate the inter-fiber failure mode in UD-FRP's. The second family of models includes those that incorporate physical aspects of fracture, often termed phenomenological or mechanistic models, such as the ones by Sun [8], Puck [9], Pinho [10], and Dávila [11]. These models do not include the interaction between longitudinal stresses and transverse stresses, but concentrate on the interaction between transverse stresses and transverse shear stresses, modeling quite well the shear strength strengthening effect during transverse compression. This second family of failure criteria was explicitly developed to predict the failure of UD-FRP.

Hence, there is still a need for a model that includes all stress interactions into one uniform equation that works for all types of anisotropic materials, such as continuous fiber, chopped fiber, and textile reinforced composite systems—a model that can be easily incorporated into finite element software in order to assess part strength. The present article derives a strength tensor based failure criteria, building on the Gol'denblat–Kopnov and Malmeister or Tsai–Wu models, which include fourth order tensor components that represent the

Correspondence to: Tim A. Osswald; e-mail: tosswald@wisc.edu
DOI 10.1002/pc.24275
Published online in Wiley Online Library (wileyonlinelibrary.com).

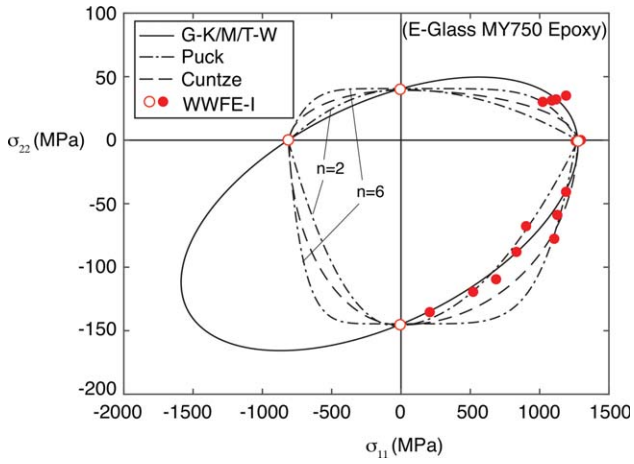

FIG. 1. Comparing the Gol'denblat–Kopnov/Malmeister/Tsai–Wu (G-K/M/T-W), Puck and Cuntze failure criteria to WWFE-I data for the $\sigma_{11}-\sigma_{22}$ failure plane. [Color figure can be viewed at wileyonlinelibrary.com]

interactions between stresses. For both failure criteria, two generalized equations are derived that describe the interactions between stresses, one for normal stress interactions, and a second for stress interactions between normal stresses and shear stresses. Finally, the new failure criterion based on the Gol'denblat–Kopnov is compared with experimental data from the literature for unidirectional fiber reinforced composite laminates, a paperboard anisotropic material and a textile-reinforced composite.

BACKGROUND

The first failure criterion for anisotropic materials appeared in Great Britain in 1948, when Hill [12] presented a model for anisotropic materials based on von Mises' distortional energy isotropic yield criteria. The 1965 Tsai adaptation of Hill's approach, now referred to as the Tsai–Hill failure criterion [3], marked the beginning of research on composites failure in the United States, and has remained one of the most widely used models to assess strength of laminated composites. While this easy to use and compact model takes into account the $\sigma_{11}-\sigma_{22}$ stress interaction, it assumes the same strength in compression as in tension, something we know is not the case with most anisotropic materials.

The same year Tsai published the Tsai-Hill failure criterion, the Russians Gol'denblat and Kopnov [4] published a strength-tensor based failure criterion where they included tensile and compressive strengths, as well as introduced the possibility of including stress interactions. However, their model only included the $\sigma_{11}-\sigma_{22}$ stress interaction. In 1966 in Latvia, Malmeister [5] modified the more general Gol'denblat-Kopnov model arriving at a somewhat simpler criterion, mostly thought of as the Tsai–Wu model [6]. In their 1971 article, Tsai and Wu [6] suggested various $\sigma_{11}-\sigma_{22}$ stress interactions, but like Gol'denblat and Kopnov and Malmeister they were silent on stress interactions between shear stresses and normal stresses. Figures 1–3 compare the Malmeister or

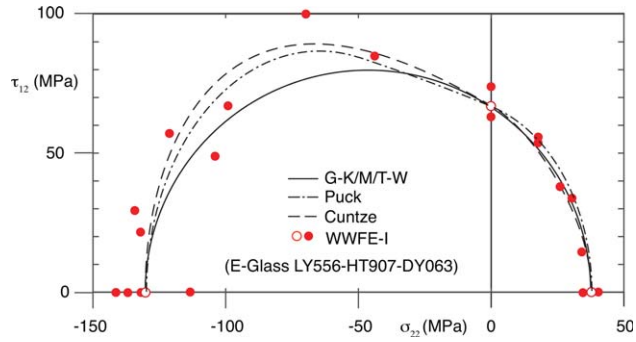

FIG. 2. Comparing the Gol'denblat–Kopnov/Malmeister/Tsai–Wu (G-K/M/T-W), Puck and Cuntze failure criteria to WWFE-I data for the $\sigma_{22}-\tau_{12}$ failure plane. [Color figure can be viewed at wileyonlinelibrary.com]

Tsai–Wu model to experimental results from the first World Wide Failure Exercise (WWFE-I) [13] in the $\sigma_{11}-\sigma_{22}$, $\sigma_{22}-\tau_{12}$, and $\sigma_{11}-\tau_{12}$ planes, respectively. With the appropriate stress interaction strength tensor component, the Gol'denblat–Kopnov model predicts the same failure surfaces as the Malmeister criterion, however, the linear nature of the scalar function f in the Gol'denblat–Kopnov criterion is more conservative and seems a more reasonable approach when modeling failure. This will be discussed in more detail in the following section.

While the Gol'denblat–Kopnov and Malmeister or Tsai–Wu models inherently reflect an increase in shear strength in the transverse compressive region (Fig. 2), they do not explicitly take the shear strengthening effect, when the composite is subjected to transverse compressive loads, into account. To account for this stress interaction, Hashin [14], Sun [8], Puck [9], Cuntze [15], Pinho [10], and Dávila [11], to name a few, developed various phenomenological approaches, where an internal Coulomb friction effect that increases the shear strength when a compressive transverse stress is applied, is included. Hashin was the first to include such an effect, by treating fiber failure and inter-fiber failure differently. With this, he laid down the groundwork for various failure criteria that followed its lead in the subsequent three decades. Sun [8] modified Hashin's criteria by adding a shear strengthening effect to the inter-fiber failure mode when compressive transverse stresses are applied. This strengthening

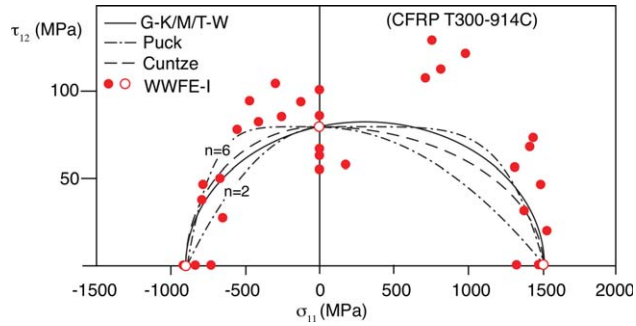

FIG. 3. Comparing the Gol'denblat–Kopnov/Malmeister/Tsai–Wu (G-K/M/T-W), Puck and Cuntze failure criteria to WWFE-I data for the $\sigma_{11}-\tau_{12}$ failure plane. [Color figure can be viewed at wileyonlinelibrary.com]

DOI 10.1002/pc

factor was included by controlling the slope of the failure surface in the $\sigma_{22}-\tau_{12}$ plane at $\sigma_{22}=0$ in the compressive transverse region, basically introducing a well defined $\sigma_{22}-\tau_{12}$ interaction. Both Hashin and Sun used a single matrix strength Y, not distinguishing between a tensile Y_t and a compressive Y_c inter-fiber failure strength, reducing the degrees of freedom when trying to fit experimental data. Furthermore, none of the models reflected an observed $\sigma_{11}-\tau_{12}$ stress interaction that leads to a shear strengthening effect observed during longitudinal tension, as presented in Fig. 3 [13].

Other well-known phenomenological models with $\sigma_{22}-\tau_{12}$ stress interactions have been developed over time. In 1996, the German composites researcher Puck [9] proposed the first true phenomenological laminate failure approach, built on his own experience in the failure of composite materials [16] and on Hashin and Sun's approaches. While Puck's "action plane" model does a very good job when including the shear strengthening effect under transverse stresses, as shown in Fig. 2, and predicting the angle of the fracture surface in the composite, the model depends on several fitting parameters that were developed specifically for the failure of unidirectional fiber reinforced laminate materials, and cannot be extended to model failure of other composites such as chopped fiber or textile reinforced composites. Puck also introduces several factors that require significant experience for its implementation and therefore make the model more difficult to use. Puck's model does not include the $\sigma_{11}-\sigma_{22}$ stress interaction and therefore, as shown in Fig. 1, does a poor job when trying to match the experimental failure surface data in the $\sigma_{11}-\sigma_{22}$ plane. Other notable failure criteria that use a phenomenological approach are the models by Pinho [10] in Great Britain, Dávila et al. [11] in the United States and Cuntze [15] in Germany. They all help in the understanding of inter-fiber failure phenomenological behavior and predict experimental measurements in the $\sigma_{22}-\tau_{12}$ plane quite well. Cuntze et al. [17] performed an extensive study on the failure of UD-FRP composites, demonstrating various effects resulting from stress interactions. Ultimately, his work led to his failure criterion that incorporates the Coulomb internal friction effect for the inter-fiber failure modes, but also couples the fiber failure and inter-fiber failure criteria [15]. Similar to the Gol'denblat–Kopnov and Malmeister or Tsai–Wu models, Cuntze's model, with a certain manipulation of tensile and compressive stresses, can be expressed with a single scalar function f, therefore coupling the failure surface to the three-dimensional stress field. Cuntze's model did not include other stress interactions, and therefore does not predict well the failure surface in the $\sigma_{11}-\sigma_{22}$ plane. The stress invariants used in Cuntze's criterion were derived for transversely isotropic composites, such as UD-FRP's, however, he has also published the stress invariants to be used when modeling transverse anisotropic materials, such as chopped fiber composites and textile reinforced composites [18].

STRENGTH TENSOR BASED FAILURE CRITERIA

The failure criterion proposed in this article is based on strength tensor based models such as the Gol'denblat–Kopnov and the Malmeister or Tsai–Wu models. The model presented by Gol'denblat and Kopnov defines a scalar failure function as a function of strength tensors and stresses using

$$f=\left(F_{ij}\sigma_{ij}\right)^{\alpha}+\left(F_{ijkl}\sigma_{ij}\sigma_{kl}\right)^{\beta}+\left(F_{ijklmn}\sigma_{ij}\sigma_{kl}\sigma_{mn}\right)^{\gamma}+\ldots \quad (1)$$

were failure is expected when $f \geq 1$. The proposed strength tensor components F_{ij}, F_{ijkl}, and F_{ijklmn} are second, fourth and sixth order tensors, respectively, that depend on engineering strength parameters such as X_t, X_c, Y_t, Y_c, and S, and satisfy the symmetry conditions, $F_{ij}=F_{ji}$ and $F_{ijkl}=F_{klij}$. However, in their analysis they only included the second and fourth order tensor terms, since higher order stress tensors, such as sixth or eighth, would increase the number of tensor components into the hundreds and thousands, respectively. To achieve a linear criterion scalar function f, Gol'denblat and Kopnov set the exponents $\alpha=1$, $\beta=1/2$, and $\gamma=1/3$. Through this additive technique Gol'denblat and Kopnov were able to couple all the failure modes into one single function, where a separate treatment of compressive and tensile modes is not required. For the plane stress case the Gol'denblat–Kopnov criterion becomes

$$\begin{aligned} f=&F_{11}\sigma_{11}+F_{22}\sigma_{22}+F_{12}\tau_{12}+(F_{1111}{\sigma_{11}}^2+F_{2222}{\sigma_{22}}^2 \\ &+F_{1212}{\tau_{12}}^2+2F_{1122}\sigma_{11}\sigma_{22}+2F_{1112}\sigma_{11}\tau_{12} \\ &+2F_{2212}\sigma_{22}\tau_{12})^{1/2} \end{aligned} \quad (2)$$

where the usual notation of σ_{ij} and τ_{ij}, for normal and shear stresses, respectively, was used. Gol'denblat and Kopnov used Eq. *2*, without the stress interaction terms F_{1112} and F_{2212}, to solve for most of the strength tensor components by assuming uniaxial conditions in the 1 and 2 directions or a shear condition in the 1–2 plane. These are all listed in Table 1. In order to determine the $\sigma_{11}-\sigma_{22}$ interaction strength tensor component F_{1122}, Gol'denblat and Kopnov measured the positive and negative shear strengths, S_{45p} and S_{45n}, of a specimen where the fibers where oriented at 45°. The resulting F_{1122} stress interaction term is also listed in Table 1.

Malmeister [5] and Tsai and Wu [6] modified the Gol'denblat–Kopnov model by letting $\alpha=1$ and $\beta=1$ from the equation, eliminating the fractional exponents, but resulting in a function f that is quadratic with respect to stress. Figure 4 illustrates this effect by comparing both models to WWFE-I data for the $\sigma_{22}-\tau_{12}$ failure plane. One can see that both models have the same failure surface, $f=1$, but by delivering a failure function f that is linear with respect to the applied stress field, the Gol'denblat–Kopnov is a more conservative approach. Furthermore, a linear function can be more easily implemented

TABLE 1. Strength tensor components for the Gol'denblat–Kopnov and the Malmeister/Tsai–Wu Failure criteria.

Tensor component	Gol'denblat–Kopnov	Malmeister/ Tsai–Wu
F_{11}	$\frac{1}{2}\left(\frac{1}{X_t}-\frac{1}{X_c}\right)$	$\frac{1}{X_t}-\frac{1}{X_c}$
F_{1111}	$\frac{1}{4}\left(\frac{1}{X_t}+\frac{1}{X_c}\right)^2$	$\frac{1}{X_tX_c}$
F_{22}	$\frac{1}{2}\left(\frac{1}{Y_t}-\frac{1}{Y_c}\right)$	$\frac{1}{Y_t}-\frac{1}{Y_c}$
F_{2222}	$\frac{1}{4}\left(\frac{1}{Y_t}+\frac{1}{Y_c}\right)^2$	$\frac{1}{Y_tY_c}$
F_{12}	0	0
F_{1212}	$\frac{1}{S^2}$	$\frac{1}{S^2}$
F_{1122}	$\frac{1}{8}\left[\left(\frac{1}{X_t}+\frac{1}{X_c}\right)^2+\left(\frac{1}{Y_t}+\frac{1}{Y_c}\right)^2-\left(\frac{1}{S_{45p}}+\frac{1}{S_{45n}}\right)^2\right]$	$\frac{f_{12}}{\sqrt{X_tX_cY_tY_c}}$

when using probabilistic failure analysis as for example proposed in the Soviet Union in 1975 by Zaitsev et al. [19] and Thieme et al. [20] in Germany in 2014. Even when using a simple factor of safety approach, in the example depicted in Fig. 4 the Gol'denblat–Kopnov criterion has no failures when using a safety factor above 1.15 ($f=0.87$), whereas the Tsai–Wu approach would still predict a failure at a safety factor of 2.1 ($f=0.47$).

Table 1 presents the strength tensor components for both the Gol'denblat–Kopnov and the Malmeister or Tsai–Wu models. The $\sigma_{11}-\sigma_{22}$ interaction strength tensor component F_{1122} proposed by Tsai and Wu [6], listed in Table 1, depends on the factor f_{12}, which lies between -1 and 0. A popular approach is letting $f_{12}=-1/2$, because it leads to the classic von Mises theory for isotropic materials [21]. However, these models neglect the longitudinal and transverse interaction terms, F_{1112} and F_{2212}, which represent the $\sigma_{11}-\tau_{12}$ and $\sigma_{22}-\tau_{12}$ interactions. These interactions, as well as a new $\sigma_{11}-\sigma_{22}$ interaction are proposed in this article and are presented in the next section.

STRESS INTERACTION STRENGTH TENSOR COMPONENTS

In this article we propose interaction strength tensor components, F_{ijkl}, based on the slopes of the failure surface ($f=1$) at any of the points where the engineering strength values are known within an arbitrary $\sigma_{ij}-\sigma_{kl}$ plane. With minimal experimental data gathered to compute the slope of the failure surface around any of the four strength values within a $\sigma_{ij}-\sigma_{kl}$ plane, the interaction strength tensor component F_{ijkl} can be evaluated. For this, we derive the interaction terms between normal stresses and the interaction between normal and shear stresses separately, as schematically depicted in Fig. 5.

To illustrate this we can take the $\sigma_{11}-\sigma_{22}$ interaction, F_{1122}, point on the failure surface where $\sigma_{11}=\sigma^u_{11-t}=X_t$ and $\sigma_{22}=0$ and the failure surface has a slope of $\frac{d\sigma_{22}}{d\sigma_{11}}=\lambda_1^{1122}$. Taking the derivative of Eq. 2 with respect to σ_{11}, at the failure surface where $f=1$ and $\tau_{12}=0$, results in

$$0=F_{11}+F_{22}\lambda_1^{1122}+\frac{1}{2}\left(F_{1111}X_t^2\right)^{-1/2}\left(2F_{1111}X_t+2F_{1122}X_t\lambda_1\right) \tag{3}$$

from which the unknown strength tensor component, F_{1122}, can be computed as

$$F_{1122}=-\frac{F_{1111}^{\frac{1}{2}}\left(F_{11}+F_{22}\lambda_1^{1122}\right)+F_{1111}}{\lambda_1^{1122}} \tag{4}$$

Finally, after substituting for F_{11}, F_{1111} and F_{22}, the $\sigma_{11}-\sigma_{22}$ strength tensor interaction term can be written as

$$F_{1122}=-\frac{1}{4}\left[\frac{2}{\lambda_1^{1122}X_t^2}+\frac{2}{\lambda_1^{1122}X_tX_c}+\frac{1}{X_tY_t}-\frac{1}{X_tY_c}+\frac{1}{X_cY_t}-\frac{1}{X_cY_c}\right] \tag{5}$$

F_{1122} can be evaluated at any of the remaining three axes intersections of the failure surface within the $\sigma_{11}-\sigma_{22}$ plane, theoretically resulting in the same computed numerical value for the strength tensor interaction term. Table 2 presents the interaction strength tensor components for the more general case where the subscripts 1122 where replaced with *iijj*.

To represent the interaction between normal stresses and shear stresses, such as F_{2212}, we assume symmetry (replacing τ_{ij} by $|\tau_{ij}|$) and propose an interaction term F_{iiij}

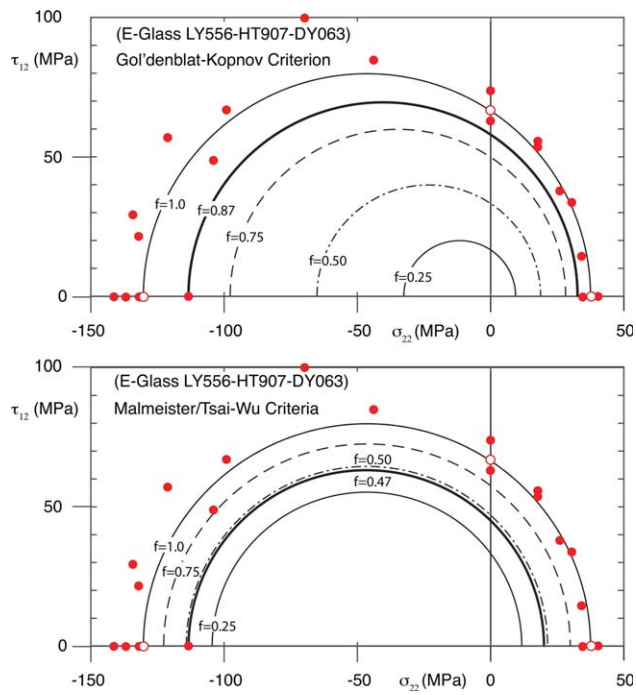

FIG. 4. Comparing the Gol'denblat–Kopnov and Malmeister or Tsai–Wu failure criteria to WWFE-I data for the $\sigma_{22}-\tau_{12}$ failure plane. [Color figure can be viewed at wileyonlinelibrary.com]

DOI 10.1002/pc

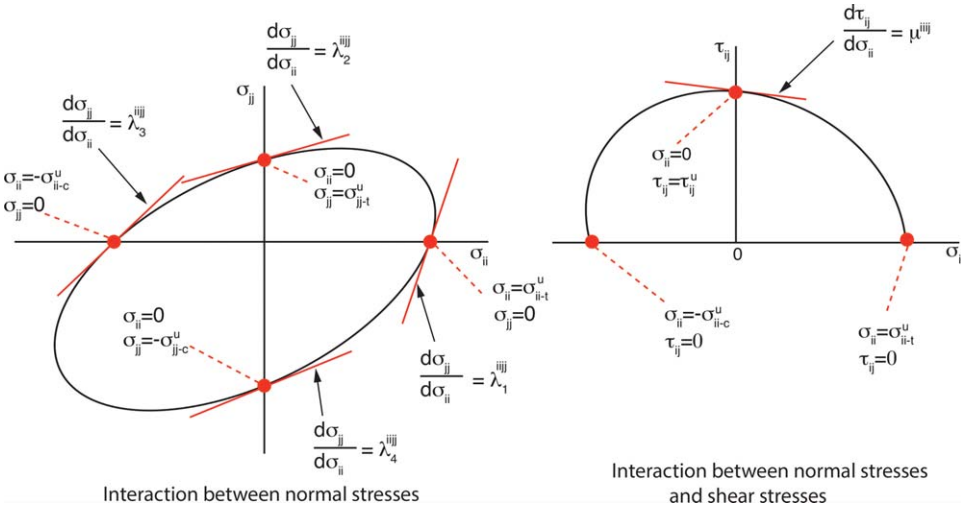

FIG. 5. Locations on the failure surface within the $\sigma_{ii}-\sigma_{jj}$ (left) and $\sigma_{ii}-\tau_{ij}$ (right) planes where the interaction F_{iijj} and F_{iiij}, respectively, can be evaluated. [Color figure can be viewed at wileyonlinelibrary.com]

based on the slope of the failure surface, $\frac{d\tau_{ij}}{d\sigma_{ii}}=\mu^{iiij}$, at $\tau_{ij}=\tau_{ij}^{u}=S$ and $\sigma_{ii}=0$, as schematically depicted in Fig. 5. For example, when deriving the F_{2212} interaction, we take the derivative of Eq. *2* with respect to σ_{22}, at the failure surface where $f=1$ and $\sigma_{22}=0$, which results in

$$0=F_{22}+\left[F_{1212}S\left(\mu^{2212}\right)+F_{2212}S\right] \tag{6}$$

where, the unknown strength tensor component, F_{2212}, can be solved for

$$F_{2212}=-\frac{F_{22}}{S}-F_{1212}\mu^{2212} \tag{7}$$

The $\sigma_{22}-\tau_{12}$ strength tensor interaction term can be written in terms of engineering strength values as

$$F_{2212}=\left[-\frac{\mu^{2212}}{S^2}-\frac{1}{2Y_tS}+\frac{1}{2Y_cS}\right] \tag{8}$$

The term is also presented in general form in Table 2 for both failure criteria.

TABLE 2. Interaction strength tensor components for the Gol'denblat–Kopnov and the Malmeister/Tsai–Wu based criteria ($\boldsymbol{\sigma}_{11-t}^{u}=X_t$, $\boldsymbol{\sigma}_{11-c}^{u}=X_c$, $\boldsymbol{\tau}_{12}^{u}=S$, etc.)

Tensor component	Gol'denblat–Kopnov	Malmeister/Tsai–Wu
$\boldsymbol{F_{iiij}}$	$-\frac{\boldsymbol{F_{ii}}}{\boldsymbol{\tau_{ij}^{u}}}-\boldsymbol{F_{ijij}}\mu^{iiij}$	$\boldsymbol{F_{ii}F_{ijij}}^{1/2}-\boldsymbol{F_{ijij}}\mu^{iiij}$
$\boldsymbol{F_{iijj}}\left(\lambda_1^{iijj}\right)$	$-\frac{\left(\boldsymbol{F_{ii}}+\boldsymbol{F_{jj}}\lambda_1^{iiij}\right)\boldsymbol{F_{iiii}}^{1/2}+\boldsymbol{F_{iiii}}}{\lambda_1^{iijj}}$	$-\frac{\boldsymbol{F_{ii}}+\boldsymbol{F_{jj}}\lambda_1^{iiij}+2\boldsymbol{F_{iiii}}\sigma_{ii-t}^{u}}{2\sigma_{ii-t}^{u}\lambda_1^{iijj}}$
$\boldsymbol{F_{iijj}}\left(\lambda_2^{iijj}\right)$	$-\left(\boldsymbol{F_{ii}}+\boldsymbol{F_{jj}}\lambda_2^{iijj}\right)\boldsymbol{F_{jjjj}}^{1/2}-\boldsymbol{F_{jjjj}}\lambda_2^{iijj}$	$-\frac{\boldsymbol{F_{ii}}+\boldsymbol{F_{jj}}\lambda_2^{iijj}+2\boldsymbol{F_{jjjj}}\sigma_{jj-t}^{u}\lambda_2^{iijj}}{2\sigma_{jj-t}^{u}}$
$\boldsymbol{F_{iijj}}\left(\lambda_3^{iijj}\right)$	$\frac{\left(\boldsymbol{F_{ii}}+\boldsymbol{F_{jj}}\lambda_3^{iijj}\right)\boldsymbol{F_{iiii}}^{1/2}-\boldsymbol{F_{iiii}}}{\lambda_3^{iijj}}$	$\frac{\boldsymbol{F_{ii}}+\boldsymbol{F_{jj}}\lambda_3^{iijj}-2\boldsymbol{F_{iiii}}\sigma_{ii-c}^{u}}{2\sigma_{ii-c}^{u}\lambda_3^{iijj}}$
$\boldsymbol{F_{iijj}}\left(\lambda_4^{iijj}\right)$	$\left(\boldsymbol{F_{ii}}+\boldsymbol{F_{jj}}\lambda_4^{iijj}\right)\boldsymbol{F_{jjjj}}^{1/2}-\boldsymbol{F_{jjjj}}\lambda_4^{iijj}$	$\frac{\boldsymbol{F_{ii}}+\boldsymbol{F_{jj}}\lambda_4^{iijj}-2\boldsymbol{F_{jjjj}}\sigma_{jj-c}^{u}\lambda_4^{iijj}}{2\sigma_{jj-c}^{u}}$

COMPARISON WITH EXPERIMENTAL DATA

The present model, based on the Gol'denblat–Kopnov criterion was compared with other models and experimental data for unidirectional FRP materials, as well as experimental data for an anisotropic paperboard and a two-ply plain weave CFRP laminate.

Unidirectional FRP

The failure of unidirectional composites in the $\sigma_{11}-\sigma_{22}$, $\tau_{12}-\sigma_{22}$, and $\tau_{12}-\sigma_{11}$ stress planes was analyzed with the present model, and compared with experiments performed with glass and carbon reinforced epoxy composites. The data was taken from the first World Wide Failure Exercise (WWFE-I) [13].

The WWFE-I fiber failure data for the $\sigma_{11}-\sigma_{22}$ plane presented in Fig. 1 was modeled using the present model using a $\lambda_4^{1112}=0.041$ and presented in Fig. 6. The resulting failure surface, $f=1$, is identical to the failure surface predicted by the Malmeister or Tsai–Wu criteria using the interaction coefficient $f_{12}=-1/2$.

The second test of the model was done with the inter-fiber failure WWFE-I data $\tau_{12}-\sigma_{22}$ stress plane used in Figs. 2 and 4. The best fit of the experimental data resulted with a parameter $\mu^{2212}=-0.77$. The present model is compared with the Gol'denblat–Kopnov and the Cuntze criteria in Fig. 7. For the Cuntze criterion $\mu_{-t}^{2212}=\mu_{-c}^{2212}=-0.55$ was used. The Cuntze "friction" parameter can be adjusted independently in tension and compression to fit the data accordingly. However, the Cuntze model misses the data points on the left of the curve. Here, the experimental data exhibits a compressive transverse strength increase that is also reflected by the present model. It is not quite clear if the compressive transverse strength increase is real. While the authors

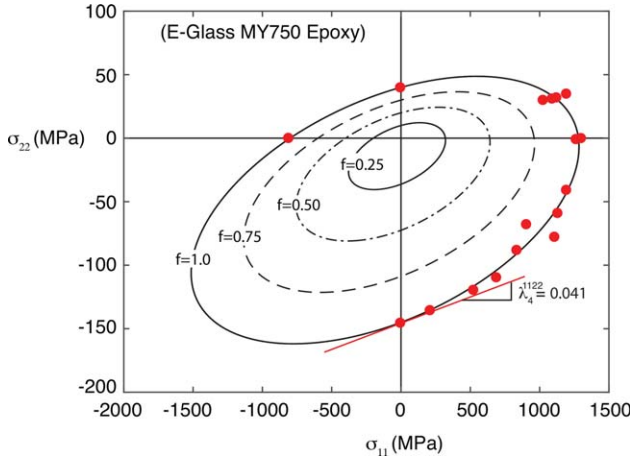

FIG. 6. Comparing the present model using $\lambda_4^{1112} = 0.041$ to WWFE-I experimental data. [Color figure can be viewed at wileyonlinelibrary.com]

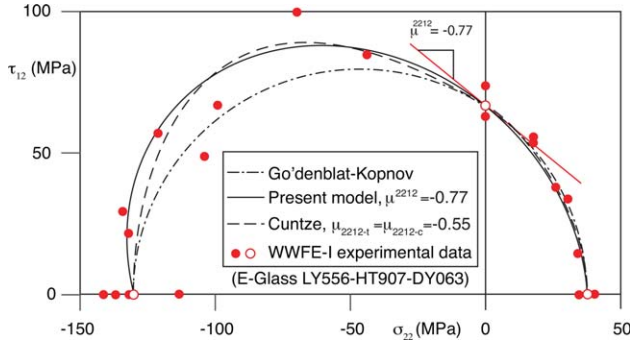

FIG. 7. Comparing the present model using $\mu^{2211} = -0.77$ to a biaxial failure stress envelope under transverse stress and shear stress loading data from the WWFE-I [13] and to the Cuntze model. [Color figure can be viewed at wileyonlinelibrary.com]

have observed this "bulge" in other experimental data [17], the literature remains silent. Figure 8, presents another set of measurements that resulted from an extensive experimental study performed by Cuntze et al. [17], and compares it to the present model and to the Cuntze criterion. The figure clearly shows how the Cuntze model captures the shear strength increase under compressive loads, but misses the compressive strength increase under shear loads. The present model is computed with two coefficients $\mu^{2212} = -0.57$ and $\mu^{2212} = -0.38$, where the first shows excellent agreement with the experimental data.

The last set of experimental data used to test the present model with unidirectional FRPC materials, is the longitudinal stress under shear stress in the $\tau_{12}-\sigma_{11}$ stress plane also used in Fig. 3. Using the present model with a parameter $\mu^{1112} = 0.054$, the shear strengthening effect under tensile longitudinal loads is clearly observed in Fig. 9.

Anisotropic Paperboard

To test the present model with an anisotropic material with a fiber orientation distribution, experiments performed on paperboard by Suhling et al. [22] were used. In their study, they found that when $\tau_{12} = 0$, the Tsai–Wu criterion with $F_{1122} = -2.297\times10^{-4}$ (MPa)$^{-1}$ gave the best fit. However, when including all four levels of shear, $\tau_{12} = 0$, $\tau_{12} = 6.9$ MPa, $\tau_{12} = 10.3$ MPa, and $\tau_{12} = 15.9$ MPa, they had to drop the longitudinal - transverse stress interaction tensor component ($F_{1122}=0$) to achieve an overall better fit. This compromised somewhat the results at $\tau_{12} = 0$, because the tilt of the elliptical failure surface and observed in the experimental results, is lost when no stress interaction exists. On the other hand, in addition to including the stress interaction strength tensor F_{1122}, the present model is able to include both shear stress–normal stress interactions F_{1112} and F_{2212}, by adjusting λ_4^{1112}, μ^{1112}, and μ^{2212}, respectively. Figure 10 compares the strength data within the $\sigma_{11}-\sigma_{22}$ stress plane at the four different shear levels to the present model. It is clear that by including all three stress

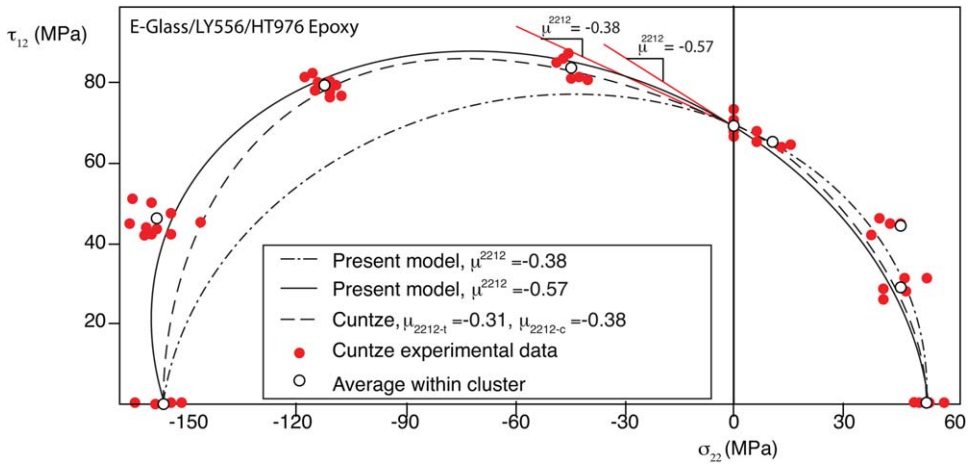

FIG. 8. Comparing the present model to a biaxial failure stress envelope under transverse stress and shear stress loading data from Cuntze et al. [17] and to the Cuntze model using $\mu^{2212} = -0.38$ and $\mu^{2212} = -0.57$. [Color figure can be viewed at wileyonlinelibrary.com]

 DOI 10.1002/pc

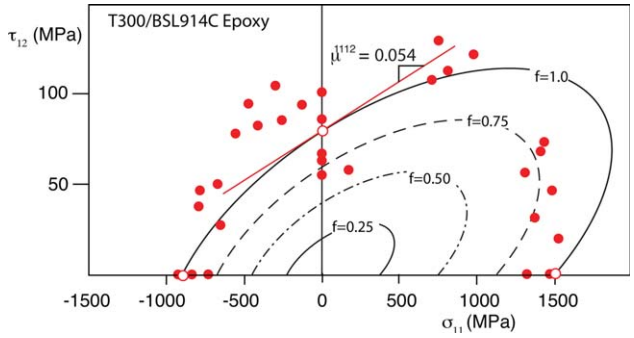

FIG. 9. Comparing the present model to WWFEI biaxial failure stress envelope data under longitudinal and shear stress loading results [13], using $\mu^{1112} = 0.054$. [Color figure can be viewed at wileyonlinelibrary.com]

interaction strength tensor components, a very good match between model and experiments was achieved.

Two-Ply Plain Weave CFRP Laminate

To validate the present model against failure data from woven fabric composite materials, experiments by Mallikarachchi and Pellegrino [23] were used. The Gol'denblat and Kopnov data presented sufficient information to show that the $\sigma_{11}-\sigma_{22}$ plane failure surface does not have a tilt and is therefore relatively circular. This is in agreement with the failure criterion developed in Greece by Theocaris [7] as well as his experimental work dealing

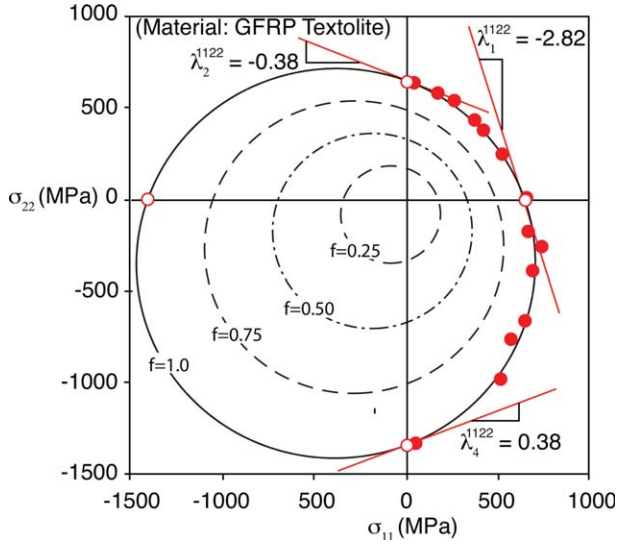

FIG. 11. Comparing the present model to biaxial in-plane strength results for a weave GFRP laminate for $\tau_{12}=0$ [4], with either $\lambda_1^{1112} = -2.82$, $\lambda_2^{1112} = -0.38$ or $\lambda_4^{1112} = 0.38$ which all give $F_{1122}=1.8\times10^{-7}$ $(\text{MPa})^{-1}$. [Color figure can be viewed at wileyonlinelibrary.com]

with weaves [24]. The present model can fit the data used in the Gol'denblat and Kopnov article very well, as can be seen in Fig. 11. There is sufficient data available to evaluate F_{1122} at three locations in the Gol'denblat and Kopnov experimental data for a textile composite [4]. The authors computed the three slopes which resulted in

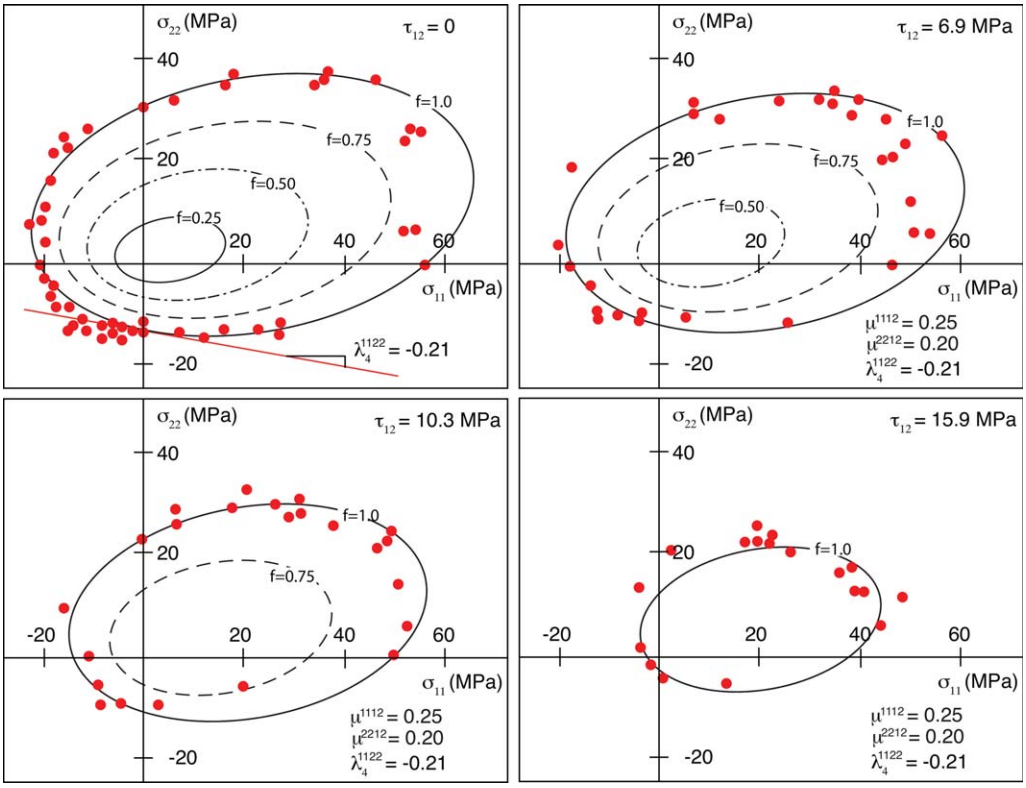

FIG. 10. Comparing the present model to biaxial in-plane strength results for paperboard experimental results [22] using $\lambda_4^{1112} = -0.21$, $\mu^{1112} = 0.25$, and $\mu^{2212} = 0.20$. [Color figure can be viewed at wileyonlinelibrary.com]

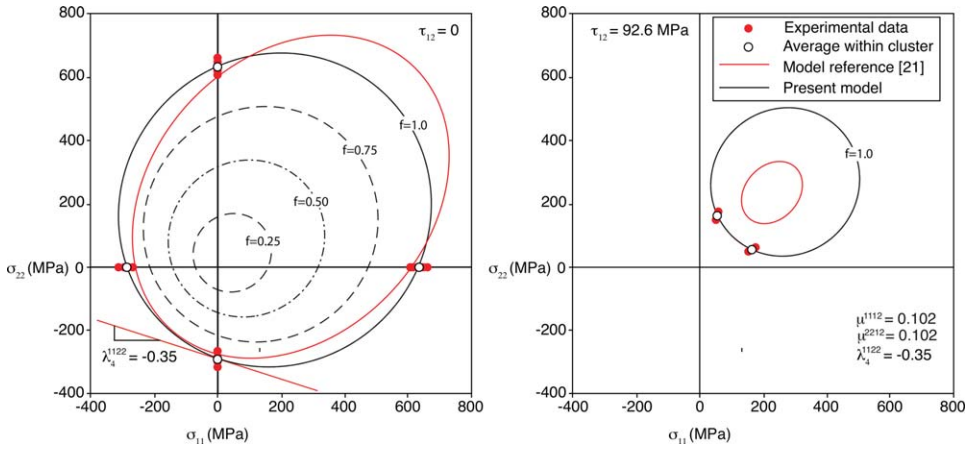

FIG. 12. Comparing the present model to biaxial in-plane strength results for a two-ply plain weave CFRP laminate for $\tau_{12}=0$ (right) and $\tau_{12}=92.6$ MPa (right) [23], with $\lambda_4^{1112}=-0.35$ and $\mu^{1112}=\mu^{2212}=0.102$. [Color figure can be viewed at wileyonlinelibrary.com]

the same longitudinal–transverse stress interaction tensor component of approximately $F_{1122}=1.8\times10^{-7}$ $(\text{MPa})^{-1}$.

To validate the present model against failure data from woven fabric composite materials with a combined longitudinal, transverse and planar shear stresses, experiments performed by Mallikarachchi and Pellegrino [23] on two-ply T300-1k/Hexcel 913 plain weave laminates were used. In their own analysis, Mallikarachchi and Pellegrino used the Tsai-Wu model with a four-fold symmetry about the third axis of the laminate, resulting in $F_{11}=F_{22}$, $F_{1112}=F_{2212}$, etc. and used Tsai-Wu's F_{1112} longitudinal - transverse stress interaction tensor component with $f_{12}=-\frac{1}{2}$. As a result, as shown in Fig. 12, their failure surface was elliptical, contradicting the findings of Gol'denblat and Kopnov [4] as well as Theocaris [24]. The present model was fit in such a way that it predicts a nearly circular failure surface by using $\lambda_4^{1112}=-0.35$. Furthermore, the parameters μ^{1112} and μ^{2212} where adjusted such that the two average data points within the $\sigma_{11}-\sigma_{22}$ failure plane, located at shear stress $\tau_{12}=92.6$, fell on the failure surface. The values of $\mu^{1112}=\mu^{2212}=0.102$ put the failure surface on top of the average values resulting in a perfect fit of the available data.

CONCLUSIONS

A strength tensor based failure criterion with stress interactions based on the Gol'denblat–Kopnov criterion was developed and tested. The proposed failure criterion with its stress interaction strength tensor components accurately predicts failure envelopes and failure trends for unidirectional fiber reinforced composite materials, as well as for anisotropic materials with a certain fiber orientation and woven fabric fiber reinforced composites. The criterion was able to capture fiber failure and inter-fiber failure phenomena for unidirectional FRP's. Furthermore, the model is able to introduce the shear strengthening effect when the unidirectional composite is subjected to longitudinal tensile loads. The model's failure surface was able to accurately predict measurements performed on an anisotropic paperboard. Finally, the proposed criterion was used to accurately predict failure within a woven carbon fiber fabric reinforced laminate. While the proposed model ignores phenomenological, micromechanical aspects of composites failure, it presents an alternative mathematically based technique, that can be easily implemented and used in conjunction with strength assessment of complex anisotropic parts.

REFERENCES

1. R. Talreja, *Compos. Sci. Technol.*, **105**, 190 (2014).
2. P.V. Osswald, Comparison of Failure Criteria of Fiber Reinforced Polymer Composites. Term Thesis, Technical University of Munich, TUM – MW65/1520 – SA, (2015).
3. S.W. Tsai, Strength characteristics of composite materials. NASA CR-224, (1965).
4. I.I. Gol'denblat and V.A. Kopnov, *Mekh. Polim.*, **1**, 70 (1965).
5. A.K. Malmeister, *Mekh. Polim.*, **4**, 519 (1966).
6. S.W. Tsai and E.M. Wu, *J. Compos. Mater.*, **5**, 58 (1971).
7. P.S. Theocaris, *Acta Mech.*, **79**, 53 (1989).
8. C.T. Sun, B.J. Quinn, and D.W. Oplinger, Comparative Evaluation of Failure Analysis Methods for Composite Laminates. DOT/FAA/AR-95/109, (1996).
9. A. Puck and H. Schürmann, *Compos. Sci. Technol.*, **58**, 1045 (1998).
10. S.T. Pinho, Modeling failure of laminated composites using physically based failure models. Ph.D. Thesis, Department of Aeronautics, Imperial College London, (2005).
11. C.G. Dávila, P.P. Camanho, and C.A. Rose, *J. Compos. Mater.*, **39**, 323 (2005).
12. R.A. Hill, *Proc. R. Soc. a*, **193**, 281 (1948).
13. P.D. Soden, M.J. Hinton, and A.S. Kaddour, *Compos. Sci. Technol.*, **62**, 1489 (2002).
14. Z. Hashin, *J. Appl. Mech.*, **47**, 329 (1980).
15. R.G. Cuntze, *Compos. Sci. Technol.*, **66**, 1081 (2006).

16. A. Puck, *Kunststoffe, German Plast*., **55**, 18 (1969) (German text 780–787).
17. R.G. Cuntze, R. Deska, B. Szelinski, R. Jeltsch-Fricker, S. Mechbach, D. Huybrechts, J. Kopp, L. Kroll, S. Gollwitzer, and R. Rackwitz, Neue Bruchkriterien und Festigkeitsnachweise für unidirektionalen Faserkunststoffverbund unter mehrachsiger Beanspruchung – Modellbildung und Experimente. VDI Fortschrittbericht. 5.506, (1997).
18. R.G. Cuntze, Aspects for achieving a reliable structural design verification? Guiding case aerospace. Großer Seminarvortrag ILK Dresden. (2005).
19. G.P. Zaitsev, V.A. Pashkov, and V.S. Strelyaev, *Moscow Aeronautical Tech. Inst*., **8**, 3 (1973).
20. M. Thieme, R. Boehm, M. Gude, and W. Hufenbach, *Compos. Sci. Technol*., **90**, 25 (2014).
21. S.W. Tsai and J.D.D. Melo, *Compos. Sci. Technol*., **123**, 71 (2016).
22. J.C. Suhling, R.E. Rowlands, M.W. Johnson, and D.E. Gunderson, *Exp. Mech*., **25**, 75 (1986).
23. H.M.Y.C. Mallikarachchi and S. Pellegrino, *J. Compos. Mater*., **47**, 1357 (2013).
24. P.S. Theocaris, *Acta Mech*., **95**, 68 (1992).